Dramatically Enhanced Photoresponse of Reduced Graphene Oxide with Linker-Free Anchored CdSe Nanoparticles

Yue Lin,[†] Kun Zhang,[†] Wufeng Chen,[‡] Yiding Liu,[§] Zhigang Geng,[†] Jie Zeng,[†] Nan Pan,[†,*] Lifeng Yan,[†] Xiaoping Wang,[†,⊥,*] and J. G. Hou[†]

[†]Hefei National Laboratory for Physical Sciences at the Microscale, [‡]Department of Chemical Physics, [§]Department of Materials Science & Engineering, and [⊥]Department of Physics, University of Science and Technology of China, Hefei, Anhui 230026, People's Republic of China

ABSTRACT A linker-free connected reduced graphene oxide/CdSe nanoparticle (R-GO/CdSe NP) nanocomposite was produced by directly anchoring CdSe NPs onto R-GO. The morphological and structural characterizations evidence that the single-crystal CdSe NPs with the size of a few tens of nanometers can be efficiently decorated on the R-GO. The photoresponse of this nanocomposite is drastically enhanced compared with that of the pure CdSe NPs, the bare R-GO, and the physically mixed R-GO/CdSe NPs, while the photoluminescence of the CdSe NPs in the composite is much quenched, indicating that the photoinduced carriers generated from the CdSe NPs can be transferred to the R-GO effectively and separately. This ability makes the R-GO/CdSe NP nanocomposite a great promise for wide potential applications in optoelectronics.

KEYWORDS: reduced graphene oxide · semiconductor nanoparticles · nanocomposite · charge transfer · photoresponse · optoelectronic

Graphene nanosheet, a kind of two-dimensional (2-D) nanostructured sp^2 carbon material, has fascinating electronic and mechanical properties due to its unique structure and is therefore highly promising for various applications such as making "paper-like" materials, batteries, hydrogen storage media, gas sensors, and even an ultrafast photodetector.[1−5] Compared to the traditional mechanical and vacuum-based preparation methods,[6,7] using graphene oxides (GO) as the starting material to produce graphene[1,8] has turned out to be an efficient, very low cost, and mass produced process. At the same time, extensive knowledge on semiconductor nanoparticles (NPs) such as CdSe, CdS, and TiO_2, whose optical and electronic properties can be tuned by controlling their size, shape, and components, has been established and developed.[9−11] It is of great interest and importance to bind these semiconductor NPs onto graphene because the combination and interaction between NPs and graphene will lead to multifunctional or even completely new properties in such a nanocomposite.[12,13]

In fact, there have been quite a few strategies on synthesizing hybrid materials based on carbon nanotubes (CNTs) and semiconductor NPs, among which two are the most popular and developed: to combine CNTs with as-synthesized NPs[14−20] or to *in situ* grow NPs onto CNTs.[21−24] However, unfortunately, the optoelectronic properties of the CNTs/NPs produced by these methods suffered from either sluggish photoresponse or restricted working condition in solution environment,[17,19,22,23] which severely hindered their applications. So far, to our best knowledge, despite the various strategies used to synthesize CNTs/NPs, there are only few reports[13,25,26] on the preparation of graphene/NP nanocomplexes. In the very limited reports, the authors attached NPs onto GO in aqueous solution, and when GO was reduced, graphene/NP was simultaneously obtained.[13,25,26] Quite recently, reduced graphene oxide (R-GO) and NPs have been successfully linked through pyridine, paving a new way to prepare R-GO/NP composite materials.[12] However, due to the indirect contact between R-GO and NPs *via* the bridging molecule, the transfer efficiency of the photoinduced carriers is still limited.

Here we report the facile synthesis of a linker-free contacted R-GO/CdSe NP nanocomposite, wherein the strategy of *in situ* growing CdSe NPs onto CNTs has been adopted.[23,24] By use of this method, satisfactorily good conductance of the nanocomposite can be obtained. Without any need of a solution environment to provide the respective transport pathways of the carriers, the R-GO/CdSe nanocomposite shows very fast and dramatically enhanced photoresponse compared to the pure CdSe NPs, the bare R-GO, the interconnected R-GO/CdSe NP solid mixture, as well as any other

*Address correspondence to npan@mail.ustc.edu.cn, xpwang@ustc.edu.cn.

Received for review January 22, 2010 and accepted May 16, 2010.

Published online May 25, 2010. 10.1021/nn100134j

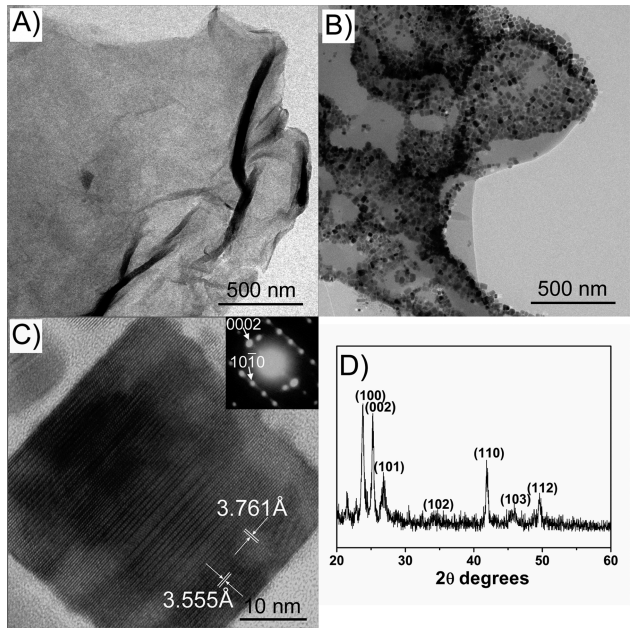

Figure 1. Representative TEM images of (A) bare R-GO and (B) R-GO/CdSe NP nanocomposite. (C) HRTEM image of an individual CdSe NP decorated on R-GO; inset shows the corresponding SAED pattern of the NP. (D) XRD 2θ scan of the R-GO/CdSe NP nanocomposite.

previously reported nanostructured carbon/NP competitors, which makes it an excellent candidate for practical optoelectronic devices especially where lightweight, compact, and flexible characteristics are needed.

RESULTS AND DISCUSSION

Figure 1A is a typical TEM image of the bare R-GO, showing that the R-GO has a sheet-like morphology with a clear, smooth surface. From the non-uniform contrast throughout the R-GO sheets, we consider that these R-GO consist of a few layers rather than monolayer graphene. XPS of the R-GO in the C1s region (Figure S1, Supporting Information) exhibits four peaks, which can be assigned to graphitic carbon atoms (284.6 eV), epoxy/ether (286.5 eV), C═O (288.5 eV), and C(O)O (289.8 eV).[2] Further analysis to the XPS result indicates that, although the R-GO still contains some oxygen-related groups, it has been clearly reduced compared to the original GO. Figure 1B is a typical TEM image of the R-GO decorated with CdSe NPs. As shown, the CdSe NPs on the R-GO are of notably high density and are mostly lying down truncated prisms (rectangular or trapezium-shaped from the top view), few nanospheres and nanorods are seen, which is rather similar to the previous result for CdSe NPs grown on SWCNTs.[24] The size of the CdSe NPs is in the range of 20−60 nm, and this broad size distribution may result from the rapid Ostwald ripening mechanism during the long growth process (4 h at 245 °C). EDS analysis reveals both signals of Se and Cd in the R-GO/CdSe nanocomposite (Figure S2, Supporting Information).

The structure of the CdSe NPs can be confirmed by the HRTEM image (Figure 1C), where the hexagonal crystalline lattice as well as some stacking faults along the ⟨0001⟩ direction can be clearly observed. The two lattice distances of 3.761 and 3.555 Å can be, respectively, indexed as $(10\bar{1}0)$ and (0002), which is consistent with the recorded SAED pattern of the CdSe NP (as shown in the inset of Figure 1C). The HRTEM and SAED results also reveal that most of the CdSe NPs are attached onto the R-GO *via* their nonpolar facets. The XRD of the R-GO/CdSe nanocomposite is shown in Figure 1D, further confirming that the CdSe NPs are of wurtzite (WZ) structure (JCPDF 77-0021). The mean grain size of the CdSe NPs calculated from the XRD peaks using the Scherrer formula is in good agreement with the TEM observation, indicating the single-crystal quality of the CdSe NPs.

Similar to the previous report on CNTs/NPs,[23] the formation of the R-GO/CdSe nanocomposite probably underwent the process where the CdSe NPs formed in solution at first and attached onto the R-GO subsequently. If the CdSe NPs are directly nucleated and grown up on R-GO, the growth rate, growth direction, and the resulted morphology will certainly differ from those of the NPs freestandingly formed in solution; however, the control experiment (where the CdSe NPs are synthesized under the same condition except that no R-GO is added) shows that the morphology, the structural details (such as the existence of the stacking faults) of the freestanding CdSe NPs, and the way they assemble are all the same as in the case of the R-GO/CdSe nanocomposite (Figure S3, Supporting Information). Therefore, we prefer to believe that the CdSe NPs are initially formed in the solvent and subsequently attach to the R-GO. It has been expected intuitively that the CdSe NPs would attach onto the R-GO *via* the Cd-rich (0001) facet as (i) Cd-rich facets can readily react with the π-system through a noncovalent bond as in the case of CNTs/CdSe,[23] and (ii) the remaining electronegative oxygen-containing groups on the R-GO (Figure S1) will also facilitate the anchoring of the CdSe NPs *via* Cd-rich facets. However, out of expectation, the CdSe NPs dominantly reside on the R-GO *via* their nonpolar facets as revealed by the HRTEM and SAED results. Nevertheless, this can also be understood by taking the electrostatic potential of the assembled CdSe NPs into account. If the CdSe NPs are side-by-side assembled and attached onto the R-GO *via* the Cd-rich (0001) facet, strong repulsive electrostatic force will exist between the adjacent Se-rich ends of the CdSe NPs as well as between the opposite Cd-rich ends, therefore making the composite unstable. However, if the CdSe NPs are end-to-end assembled and bonded onto the R-GO *via* nonpolar facets, the extra electrostatic potential can be eliminated; the π-system and oxygen-containing groups in the R-GO can also react with the Cd atoms on the nonpolar facets of the CdSe NPs. Therefore, it is reasonable that the

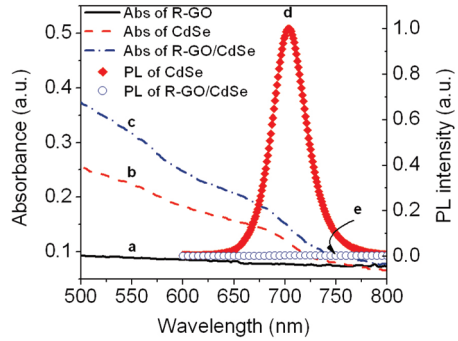

Figure 2. Absorption spectra of bare R-GO (curve a), pure CdSe NPs (curve b), and R-GO/CdSe NP nanocomposite (curve c) as well as the corresponding PL spectra (excited at 370 nm) of the pure CdSe NPs (curve d) and the nanocomposite (curve e).

CdSe NPs anchor on the R-GO *via* nonpolar facets, which differs from the CNT/CdSe composite.

By this method, we can decorate CdSe NPs onto both sides of R-GO, as shown in Figure S4 (Supporting Information). In addition, the adhesion and stability against ultrasonication of the CdSe NPs on the R-GO can be controlled and improved by increasing the growth time. Only if the growth time is less than 0.5 h, will the small CdSe NPs be occasionally removed from the R-GO during the ultrasonic bath. We believe that the distance between the CdSe NPs and the adjacent R-GO would also be atomically close as the literature has reported.[23] At present, we do not know the exact reason for the stacking fault formation in the CdSe NPs, and more efforts are to be made in the future to elucidate this behavior.

Figure 2 shows the absorption spectra of the R-GO/CdSe nanocomposite as well as those of the bare R-GO and the pure CdSe NPs. As shown, the bare R-GO only has weak and featureless absorption in the 500−800 nm region (curve a) as the reported result.[27] The absorption spectra of the pure CdSe NPs (synthesized at the same condition except the absence of R-GO) with the average size of ~20 nm (curve b) are similar to that of the R-GO/CdSe nanocomposite (curve c), displaying two main peaks centered around 564 and 685 nm. The absorption peaks red shift significantly compared with those of the 4 nm CdSe NPs;[12] this is reasonable since the sizes of the CdSe NPs here are much larger than the exciton Bohr radius of CdSe (5.6 nm).[28]

The PL spectra of the R-GO/CdSe nanocomposite and the corresponding pure CdSe NPs dispersed in toluene are also shown in Figure 2. As seen, a dominant emission peak at ~704 nm (fwhm ~41.7 nm) can be clearly observed for the pure CdSe NPs (curve d), while the PL of the R-GO/CdSe nanocomposite is too weak to be identified (curve e). Similar to the previous reports on other semiconductor NP/carbon-based nanostructures,[17,22,25,29−31] this behavior can be attributed to the fact that the photoinduced electrons and holes in the CdSe NPs prefer separately transferring to

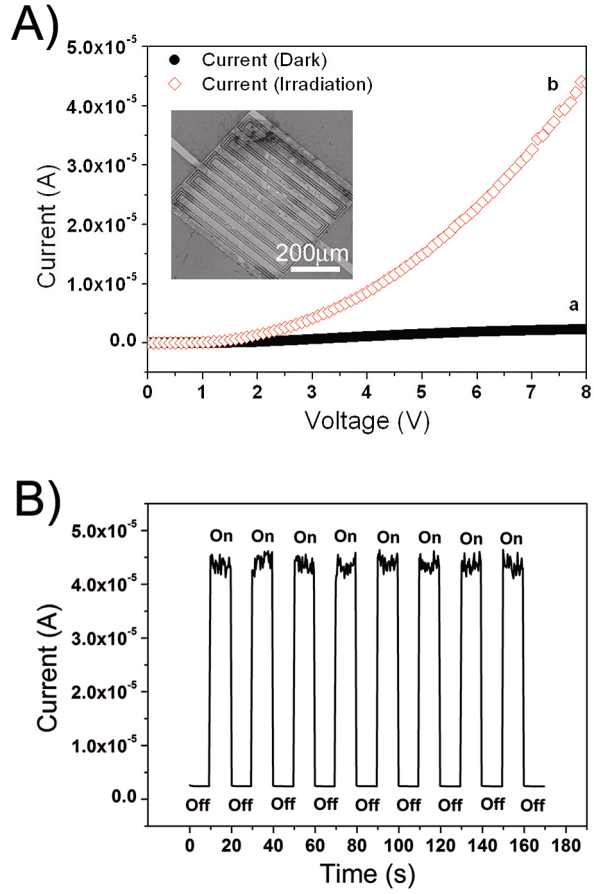

Figure 3. (A) Typical *I*−*V* characteristic of the R-GO/CdSe NP nanocomposite without (curve a) and with irradiation (curve b); inset is the corresponding SEM image of the sample after being drop-cast onto a gold interdigital electrode. (B) Current response *versus* time under chopped irradiation (under a bias voltage of 8 V).

the R-GO. As a consequence, the radiative recombination of the electron−hole pairs is hampered and the PL is quenched significantly.

Due to the efficient transfer of the photoinduced carriers from CdSe NPs to R-GO, one can expect that an enhanced photoresponse will occur in the R-GO/CdSe NP nanocomposite. Therefore, photoresponse is measured on a prototype photodetector device fabricated by drop casting the R-GO/CdSe NP nanocomposite dispersed in toluene onto a gold interdigital electrode on SiO_2 substrate with a 4.5 μm spacing between the adjacent fingers (inset in Figure 3A). Figure 3A shows the typical *I*−*V* curves of the device without and with the irradiation of a continuous wave laser (excitation at $\lambda = 532$ nm with an optical power of 12 mW). As shown, the current is drastically increased when the irradiation is on. The photosensitivity of the R-GO/CdSe nanocomposite, defined as the ratio of the current under the irradiation to that under the dark, can be as large as ~1700%, which is dramatically increased compared to the result of 9.1% in the recent report.[12] It is also worth mentioning that the photocurrent response of the R-GO/CdSe nanocomposite is fairly re-

versible and stable, and the related result at a bias of 8 V under several on/off irradiation cycles is shown in Figure 3B, from which we can see that the current can reproducibly increase violently under each irradiation and recover rapidly in the dark.

The control experiments have been performed on both the pure CdSe NPs and the bare R-GO. As is shown in Figures S5 and S6 (Supporting Information), the pure CdSe NPs only show a very weak photoresponse and the bare R-GO shows no photoresponse, respectively, which clearly confirms that the enhanced photoresponse of the nanocomposite is due to the synergy of the R-GO and the CdSe NPs. Another control experiment was also carried out where the CdSe NPs were simply dropped onto the R-GO and dried (the morphology of the solid mixture between the electrodes has been verified by SEM, as shown in Figure S7). It is revealed that, in the case of the R-GO/CdSe NP solid mixture, the photoresponse is still very weak, as shown in Figure S8.

All of the above results strongly evidence that the dramatically enhanced photoresponse is primarily, if not all, benefited from the robust combination and good interfacial quality built between the CdSe NPs and R-GO in the nanocomposite, which greatly facilitate the transfer of the photoinduced carriers. This is also consistent with the recent report where the CdSe and R-GO were combined through a molecular linker instead of direct contact,[12] and the photosensitivity was therefore notably degraded. It should be stressed that our R-GO/CdSe NP nanocomposite through direct contact between the NPs and the R-GO also possesses an extremely short photoresponse time. Its response time to the irradiation on and off can be, respectively, less than 250 and 500 μs (see Figures S9 and S10 in the Supporting Information), much shorter than that of the reported R-GO/NP composite connected *via* molecular linker.[12] We also find that the photoresponse of the R-GO/CdSe NP nanocomposite is insensitive to the ambient pressure. As shown in Figure S11, the photocurrent only decreases by less than 0.7% when the pressure changes from 10^5 to 320 Pa, and the repeatability of the photoresponse at 320 Pa is also reserved.

Among the reports on carbon-based nanostructures decorated with semiconductor NPs, in some cases, the charge separation was implemented in solution, where electrons were transferred into carbon-based nanostructures while holes were captured by a sacrificial donor such as triethanolamine,[22] ethanol,[17,25,29] and Na_2S electrolyte;[31] in other cases, the process was not restricted in solution; however, once electrons were transferred to carbon-based nanostructures, holes will stay and accumulate in semiconductor NPs, prolonging the response time to more than hundreds of seconds.[19,23,30] The most recently reported R-GO/NP composite, attached *via* a bridging molecule, has a relatively fast response of several seconds.[12] As a comparison, the directly attached R-GO/CdSe NP nanocomposite shown here holds a very fast photoresponse time as short as ≤250 μs, which is much shorter than that of any other nanostructured carbon/NP competitors. Especially, in contrast with the CNT/CdSe NP composite, the gate effect that resulted from the accumulated holes in the CdSe NPs is absent here despite the similarity between the two systems. Therefore, we believe that both the drastic enhancement in the photoresponse and the quenching in PL are due to the efficient and separate transfer of the photoinduced charges from the CdSe NPs to the R-GO. For a better understanding of this phenomenon, the energy band structure near the interface between the CdSe and the R-GO should be considered. Since the band gap of WZ CdSe is 1.8 eV[32] and its valence band maximum (VBM) is ~6.3 eV,[33] one can derive a conduction band minimum (CBM) of ~4.5 eV, while the location of VBM and CBM of R-GO can be roughly estimated to 4.66−4.71 and 4.61−4.66 eV, respectively, by considering the graphene's work function of ~4.66 eV[34] and the small opened gap of 10−50 meV possibly remained in the R-GO caused by the incomplete reduction.[35] As a result, when the CdSe is directly and tightly contacted with the R-GO, a large valence band offset will form at the R-GO/CdSe interface while the conduction band offset is very small. Once the photoinduced electrons and holes are generated in the CdSe, they will most likely transfer to the R-GO owing to the energy band offsets at the interface. However, their transfer rates are probably entirely different due to the distinctly different energy band offsets at the interface, which means that the electrons and holes will probably transfer to the R-GO separately. These electrons and holes transferred into the R-GO will soon be drifted to the opposite electrodes of the device by the external electric field,[5] thus accounting for the dramatically enhanced photoresponse.

In addition, the photocurrent response *versus* the irradiation power under different bias voltages has been studied. As shown in Figure S12 (Supporting Information), a characteristic saturation behavior of the photocurrent response with the increased irradiation power can be found despite the various applied bias voltages. This saturation behavior can be attributed to the nonlinear absorption of the CdSe NPs (the effective absorption of the NP becomes saturated as the power of irradiation continuously increases).[36] If the quantities of the photon-generated electrons and holes in a CdSe NP are large enough, they can readily fill up the states in the CB and VB of the NP, hindering the electrons and the holes from further filling into these states owing to the Pauli exclusion principle and therefore saturating the effective absorption.[37] Since the carriers are created by the photons absorbed, such a saturation in the absorption certainly leads to the saturation in the photocurrent. However, if the bias voltage is increased (from 4 to 6 V and then to 8

V), the critical irradiation (defined as the power over which the photocurrent begins to show saturated behavior) power slightly shifts to the larger value. This can also be well-understood as follows: the external electric field becomes stronger with the higher applied bias voltage, and this stronger electric field promotes the transfer of the photoexcited electrons and holes from the CdSe NP to the R-GO, releasing more occupied energy states in the NP so that more (originally surplus) photoexcited carriers can be accommodated and become contributive to the photocurrent; therefore, a shift of the critical power to the larger value is observed.

Besides the photosensitivity and the response rate, the stability of the nanocomposites is also quite important for the practical device applications. For this reason, the stability of the R-GO/CdSe NP nanocomposites has been evaluated by remeasuring the photoresponse of the same prototype device after the exposure to open air for 270 days. As shown, the photosensitivity (Figure S13, Supporting Information) and the photoresponse rate (Figures S14 and S15) of the device can be well-maintained after 270 day exposure to the open air environment. Such an exceptionally good stability clearly demonstrates the capability and feasibility of this R-GO/CdSe NP nanocomposite to be used as practical photodetector devices.

CONCLUSION

In conclusion, R-GO/CdSe NP nanocomposite is prepared *via* adding R-GO into the reaction solution during the process of synthesizing CdSe NPs, by which the CdSe NPs are directly anchored onto the R-GO. As compared with the bare R-GO, the pure CdSe NPs, and the physically mixed R-GO/CdSe NPs, the R-GO/CdSe NP nanocomposite possesses a dramatically enhanced photoresponse with very fast response time, outmatching the performance of any other nanostructured carbon/NP competitors that have been reported. This behavior can be interpreted by the efficient and separate transfer of the photoinduced carriers from the CdSe NPs to the R-GO. The good ability to enhance photoinduced charge transfer makes this R-GO/CdSe NP nanocomposite extraordinarily promising in optoelectronic device applications especially where lightweight, compact, and flexible characteristics are needed.

MATERIALS AND METHODS

Chemicals. Cadmium stearate ($Cd(SA)_2$, 90%) was purchased from Wako Pure Chemical Industries, Ltd. Hexadecanediol (HDA, ≥90%) and trioctylphosphine (TOP, 90%) were purchased from Fluka. Tri-*n*-octylphosphine oxide (TOPO, 98%) was purchased from Alfa Aesar. Se powder (≥99.95%) and 1,2-dichloroethane (DCE, ≥99%) were purchased from Shanghai Meixing Chemical Co., Ltd. and Sinopharm Chemical Reagent Co., Ltd., respectively. All chemicals were used without further purification.

Synthesis of the R-GO/CdSe Nanocomposite. Graphite oxide (GO) was synthesized through Hummers method.[25] To obtain R-GO, the as-synthesized GO was reduced in hydrazine and ammonia solution at room temperature for 1 day.[2] R-GO/CdSe nanocomposites were synthesized by adding R-GO directly into the reaction solution during the process of synthesizing CdSe NPs.[23,24,38,39] In a typical synthesis, first, 0.2 mmol $Cd(SA)_2$ mixed with 2 g of HDA and 2 g of TOPO was slowly increased to 80 °C under nitrogen protection. After the $Cd(SA)_2$/HDA/TOPO solution reached and was kept at 80 °C for 5 min, 0.4 mg of R-GO, which had been dispersed in 100 μL of DCE and ultrasonicated for 0.5 h, was then injected. After 5 min of stirring, the suspension temperature was increased to 100 °C, followed by a vessel degassing process for 3 min. After that, the suspension was heated to 255 °C, in a moment, 0.5 mmol Se powder predissolved in 2 mL of TOP under ultrasonication was injected into the suspension. The color of the suspension became brown gradually. After 1 min, the temperature was set to and then kept at 245 °C for 4 h. After cooling, the as-synthesized R-GO/CdSe nanocomposites were finally purified by ultrasonication and centrifugation in toluene three times.

Characterization. The product was characterized by various techniques. Scanning electron microscopy (SEM) was conducted on a Sirion 200 FESEM at an accelerating voltage of 10 kV. High-resolution transmission electron microscopy (HRTEM), selected area electron diffraction (SAED), and energy-dispersive spectroscopy (EDS) were conducted on a JEOL-2011 operated at 200 kV. X-ray diffraction (XRD) was carried out on a MAC MXPAHF X-ray diffractometer with Cu Kα line (λ = 1.54056 Å). X-ray photoelectron spectroscopy (XPS) was performed on an ESCALAB 250 (Thermo-VG Scientific). UV−vis absorption spectra were obtained on a U-4100 spectrophotometer (HITACHI). Photoluminescence (PL) was collected on Fluorolog3-TAU. Electrical experiments were performed at room temperature using a Keithley-4200 instrument. The laser source used in the photoresponse detection was DPGL-3020LI (Photop Suwtech, Inc.) with a wavelength of 532 nm, whose power was measured as 12mW using a LCP-33 laser checker (SIGMA KOKI).

Acknowledgment. We thank Mr. Liuguo Chen and Professor Zhenchao Dong of USTC for helpful discussions and experimental support. This work is supported by the National Natural Science Foundation of China (NSFC) under Grant Nos. 50721091, 10874165, and 90921013 as well as by CAS and MOST (2006CB922002) of China. N.P. also thanks the China Postdoctoral Science Foundation (20090460737) and the Fundamental Research Funds for the Central Universities (FRFCU) for support.

Supporting Information Available: Figures S1−S15. This material is available free of charge *via* the Internet at http://pubs.acs.org.

REFERENCES AND NOTES

1. Li, D.; Muller, M. B.; Gilje, S.; Kaner, R. B.; Wallace, G. G. Processable Aqueous Dispersions of Graphene Nanosheets. *Nat. Nanotechnol.* **2008**, *3*, 101–105.
2. Park, S.; Lee, K.-S.; Bozoklu, G.; Cai, W.; Nguyen, S. T.; Ruoff, R. S. Graphene Oxide Papers Modified by Divalent Ions-Enhancing Mechanical Properties *via* Chemical Cross-Linking. *ACS Nano* **2008**, *2*, 572–578.
3. Dikin, D. A.; Stankovich, S.; Zimney, E. J.; Piner, R. D.; Dommett, G. H. B.; Evmenenko, G.; Nguyen, S. T.; Ruoff, R. S. Preparation and Characterization of Graphene Oxide Paper. *Nature* **2007**, *448*, 457–460.
4. Schedin, F.; Geim, A. K.; Morozov, S. V.; Hill, E. W.; Blake, P.; Katsnelson, M. I.; Novoselov, K. S. Detection of Individual Gas Molecules Adsorbed on Graphene. *Nat. Mater.* **2007**, *6*, 652–655.
5. Xia, F.; Mueller, T.; Lin, Y.-m.; Valdes-Garcia, A.; Avouris, P. Ultrafast Graphene Photodetector. *Nat. Nanotechnol* **2009**, *4*, 839–843.
6. Novoselov, K. S.; Geim, A. K.; Morozov, S. V.; Jiang, D.; Zhang, Y.; Dubonos, S. V.; Grigorieva, I. V.; Firsov, A. A.

Electric Field Effect in Atomically Thin Carbon Films. *Science* **2004**, *306*, 666–669.
7. Li, X.; Cai, W.; An, J.; Kim, S.; Nah, J.; Yang, D.; Piner, R.; Velamakanni, A.; Jung, I.; Tutuc, E.; *et al.* Large-Area Synthesis of High-Quality and Uniform Graphene Films on Copper Foils. *Science* **2009**, *324*, 1312–1314.
8. Eda, G.; Fanchini, G.; Chhowalla, M. Large-Area Ultrathin Films of Reduced Graphene Oxide as a Transparent and Flexible Electronic Material. *Nat. Nanotechnol.* **2008**, *3*, 270–274.
9. Murray, C. B.; Norris, D. J.; Bawendi, M. G. Synthesis and Characterization of Nearly Monodisperse CdE (E = S, Se, Te) Semiconductor Nanocrystallites. *J. Am. Chem. Soc.* **1993**, *115*, 8706–8715.
10. Jun, Y. W.; Casula, M. F.; Sim, J. H.; Kim, S. Y.; Cheon, J.; Alivisatos, A. P. Surfactant-Assisted Elimination of a High Energy Facet as a Means of Controlling the Shapes of TiO_2 Nanocrystals. *J. Am. Chem. Soc.* **2003**, *125*, 15981–15985.
11. Manna, L.; Scher, E. C.; Alivisatos, A. P. Synthesis of soluble and Processable Rod-, Arrow-, Teardrop-, and Tetrapod-Shaped CdSe Nanocrystals. *J. Am. Chem. Soc.* **2000**, *122*, 12700–12706.
12. Geng, X.; Niu, L.; Xing, Z.; Song, R.; Liu, G.; Sun, M.; Cheng, G.; Zhong, H.; Liu, Z.; Zhang, Z.; *et al.* Aqueous-Processable Noncovalent Chemically Converted Graphene-Quantum Dot Composites for Flexible and Transparent Optoelectronic Films. *Adv. Mater.* **2010**, *22*, 638–642.
13. Cao, A.; Liu, Z.; Chu, S.; Wu, M.; Ye, Z.; Cai, Z.; Chang, Y.; Wang, S.; Gong, Q.; Liu, Y. A Facile One-Step Method To Produce Graphene−CdS Quantum Dot Nanocomposites as Promising Optoelectronic Materials. *Adv. Mater.* **2009**, *22*, 103–106.
14. Banerjee, S.; Wong, S. S. Synthesis and Characterization of Carbon Nanotube−Nanocrystal Heterostructures. *Nano Lett.* **2002**, *2*, 195–200.
15. Sheeney-Haj-Ichia, L.; Basnar, B.; Willner, I. Efficient Generation of Photocurrents by Using CdS/Carbon Nanotube Assemblies on Electrodes. *Angew. Chem., Int. Ed.* **2005**, *44*, 78–83.
16. Olek, M.; Busgen, T.; Hilgendorff, M.; Giersig, M. Quantum Dot Modified Multiwall Carbon Nanotubes. *J. Phys. Chem. B* **2006**, *110*, 12901–12904.
17. Kongkanand, A.; Kamat, P. V. Electron Storage in Single Wall Carbon Nanotubes. Fermi Level Equilibration in Semiconductor−SWCNT Suspensions. *ACS Nano* **2007**, *1*, 13–21.
18. Lu, C.; Akey, A.; Wang, W.; Herman, I. P. Versatile Formation of CdSe Nanoparticle−Single Walled Carbon Nanotube Hybrid Structures. *J. Am. Chem. Soc.* **2009**, *131*, 3446–3447.
19. Li, X.; Jia, Y.; Cao, A. Tailored Single-Walled Carbon Nanotube−CdS Nanoparticle Hybrids for Tunable Optoelectronic Devices. *ACS Nano* **2010**, *4*, 506–512.
20. Liu, S.; Ye, J.; Cao, Y.; Shen, Q.; Liu, Z.; Qi, L.; Guo, X. Tunable Hybrid Photodetectors with Superhigh Responsivity. *Small* **2009**, *5*, 2371–2376.
21. Na, Y. J.; Kim, H. S.; Park, J. Morphology-Controlled Lead Selenide Nanocrystals and Their *In Situ* Growth on Carbon Nanotubes. *J. Phys. Chem. C* **2008**, *112*, 11218–11226.
22. Robel, I.; Bunker, B. A.; Kamat, P. V. Single-Walled Carbon Nanotube−CdS Nanocomposites as Light-Harvesting Assemblies: Photoinduced Charge-Transfer Interactions. *Adv. Mater.* **2005**, *17*, 2458–2463.
23. Jua'rez, B. H.; Klinke, C.; Kornowski, A.; Weller, H. Quantum Dot Attachment and Morphology Control by Carbon Nanotubes. *Nano Lett.* **2007**, *7*, 3564–3568.
24. Jua'rez, B. H.; Meyns, M.; Chanaewa, A.; Cai, Y.; Klinke, C.; Weller, H. Carbon Supported CdSe Nanocrystals. *J. Am. Chem. Soc.* **2008**, *130*, 15282–15284.
25. Williams, G.; Seger, B.; Kamat, P. V. TiO_2-Graphene Nanocomposites. UV-Assisted Photocatalytic Reduction of Graphene Oxide. *ACS Nano* **2008**, *2*, 1487–1491.
26. Williams, G.; Kamat, P. V. Graphene−Semiconductor Nanocomposites: Excited-State Interactions between ZnO Nanoparticles and Graphene Oxide. *Langmuir* **2009**, *25*, 13869–13873.
27. Hernandez, Y.; Nicolosi, V.; Lotya, M.; Blighe, F. M.; Sun, Z.; De, S.; McGovern, I. T.; Holland, B.; Byrne, M.; Gun'Ko, Y. K.; *et al.* High-Yield Production of Graphene by Liquid-Phase Exfoliation of Graphite. *Nat. Nanotechnol.* **2008**, *3*, 563–568.
28. Zhong, X.; Feng, Y.; Knoll, W.; Han, M. Alloyed $Zn_xCd_{1-x}S$ Nanocrystals with Highly Narrow Luminescence Spectral Width. *J. Am. Chem. Soc.* **2003**, *125*, 13559–13563.
29. Kamat, P. V.; Bedja, I.; Hotchandani, S. Photoinduced Charge Transfer between Carbon and Semiconductor Clusters. One-Electron Reduction of C_{60} in Colloidal TiO_2 Semiconductor Suspensions. *J. Phys. Chem.* **1994**, *98*, 9137–9142.
30. Biebersdorf, A.; Dietmuller, R.; Susha, A. S.; Rogach, A. L.; Poznyak, S. K.; Talapin, D. V.; Weller, H.; Klar, T. A.; Feldmann, J. Semiconductor Nanocrystals Photosensitize C_{60} Crystals. *Nano Lett.* **2006**, *6*, 1559–1563.
31. Brown, P.; Kamat, P. V. Quantum Dot Solar Cells. Electrophoretic Deposition of CdSe−C_{60} Composite Films and Capture of Photogenerated Electrons with nC_{60} Cluster Shell. *J. Am. Chem. Soc.* **2008**, *130*, 8890–8891.
32. Efros, A. L.; Rosen, M. The Electronic Structure of Semiconductor Nanocrystals. *Annu. Rev. Mater. Sci.* **2000**, *30*, 475–521.
33. Hagfeldt, A.; Graetzel, M. Light-Induced Redox Reactions in Nanocrystalline Systems. *Chem. Rev.* **1995**, *95*, 49–68.
34. Shan, B.; Cho, K. First Principles Study of Work Functions of Single Wall Carbon Nanotubes. *Phy. Rev. Lett.* **2005**, *94*, 236602.
35. Eda, G.; Mattevi, C.; Yamaguchi, H.; Kim, H.; Chhowalla, M. Insulator to Semimetal Transition in Graphene Oxide. *J. Phys. Chem. C* **2009**, *113*, 15768–15771.
36. Park, S. H; Casey, M. P.; Falk, J. Nonlinear Optical Properties of CdSe Quantum Dots. *J. Appl. Phys.* **1993**, *73*, 8041–8045.
37. Schmitt-Rink, S.; Miller, D. A. B.; Chemla, D. S. Theory of the Linear and Nonlinear Optical Properties of Semiconductor Microcrystallites. *Phys. Rev. B* **1987**, *35*, 8113–8125.
38. Zeng, J.; Liu, C.; Huang, J.; Wang, X.; Zhang, S.; Li, G.; Hou, J. UV-Light Induced Fabrication of $CdCl_2$ Nanotubes through CdSe/Te Nanocrystals Based on Dimension and Configuration Control. *Nano Lett.* **2008**, *8*, 1318–1322.
39. Zeng, J.; Lu, W.; Wang, X.; Wang, B.; Wang, G.; Hou, J. Fine Tuning Photoluminescence Properties of CdSe Nanoparticles by Surface States Modulation. *J. Colloid Interface Sci.* **2006**, *298*, 685–688.